

Optimization of the atom interferometer phase produced by the set of cylindrical source masses to measure the Newtonian gravity constant

B. Dubetsky*

1849 S Ocean Dr, Apt 207, Hallandale, FL 33009

(Dated: September 19, 2019)

An analytical expression for the gravitational field of a homogeneous cylinder is derived. The phase of the atom interferometer produced by the gravity field of the set of cylinders has been calculated. The optimal values of the initial positions and velocities of atomic clouds were obtained. It is shown that at equal sizes of the atomic cloud in the vertical and transverse directions, as well as at equal atomic vertical and transverse temperatures, systematic errors due to the finite size and temperature of the cloud disappear. To overcome the influence of the Earth gravitational field on the accuracy of the phase double difference measurement, it is proposed to use the technique of eliminating gravity-gradient terms. After eliminating, one can use extreme values of the atomic positions and velocities. Nonlinear dependences of the phase on the uncertainties of atomic positions and velocities near those extreme values required us to modify the expression for the standard phase deviation. Moreover, such dependences lead to a phase shift, which was also calculated. The relative accuracy of measurements of Newtonian gravitational constant 10^{-4} and $2 \cdot 10^{-5}$ is predicted for sets of 24 and 630 cylinders, respectively.

PACS numbers: 03.75.Dg; 37.25.+k; 04.80.-y

*Electronic address: bdubetsky@gmail.com

I. INTRODUCTION.

Atom interferometry [1] is now used to measure Newtonian gravity constant G [2–4]. Searches for new schemes and options promise to increase the accuracy of these measurements. Previously, it was shown [5] that, in principle, the current state-of-art in atom interferometry would allow one to measure G with an accuracy of 200ppb. To achieve such a goal one has to use *simultaneously* the largest time delay between pulses $T = 1.15$ s [6], temperature 115pK and radius of the atom cloud 170μ (which are larger than those observed in [7]), the beam splitter with an effective wave vector $k = 8.25 \cdot 10^8 \text{ m}^{-1}$ [8], the source mass 1080kg [9] and phase noise $\phi_{err} = 10^{-4}\text{rad}$. The following procedure was used [3–5, 10]. The source mass consists of two halves, which are placed in two different configurations C and F. We accept the notation "C and F," which was previously used in articles [3, 4]. The atomic gradiometer [11] measures the phase difference of two atomic interferometers (AIs) 1 and 2

$$\Delta\phi^{(C,F)} = \phi^{(C,F)}(z_1, v_{z_1}) - \phi^{(C,F)}(z_2, v_{z_2}), \quad (1)$$

where $\phi^{(C,F)}(z_j, v_j)$ is the phase of AI j , in which the atoms are launched vertically from point $\mathbf{x}_j = (0, 0, z_j)$ at velocity $\mathbf{v}_j = (0, 0, v_{z_j})$. Phase difference (1) consists of two parts, the one that is induced by the gravitational field of the Earth and inertial terms and the one that is associated with the gravitational field of the source mass. One expects [2–4] that the phase double difference (PDD)

$$\Delta^2\phi = \Delta\phi^{(C)} - \Delta\phi^{(F)} \quad (2)$$

will depend only on the AI phase $\phi_s^{(C,F)}(z_j, v_j)$ produced only by the field of source mass, and therefore can be used to measure the Newtonian gravitational constant G . Despite the fact that the gravitational field of the Earth does not affect the PDD, the gradient of this field affects [3, 4] on the accuracy of the PDD measurement. In article [3, 4], to reduce this influence, the mutual position of the source mass and atomic clouds are selected so that at the point of apogee of the atomic trajectories gradients of the Earth's field and the field of the source mass cancel each other. Below in Sec. IV we will see that this technique only partially reduces the influence of the gravitational field of the Earth on the accuracy of the G measurement.

To resolve this problem we suggest using the method of eliminating the sensitivity of the phase to the atom position and velocity [12], which is achieved by changing the wave vector of the second Raman pulse, so that

$$\mathbf{k}_2 = \mathbf{k} + \frac{1}{2}\Gamma_E T^2 \mathbf{k}, \quad (3)$$

where Γ_E is gravity-gradient tensor of the Earth field. The possibility of using the technique of [12] for measuring G was considered by G. Rosi [13]. The difference from what is proposed here is that we propose to eliminate only the gradient of the gravitational field of the Earth. Since the gravity gradient tensor is measured with some accuracy $\delta\Gamma_E$, it still contributes to the error budget. One can ignore this influence if the relative standard deviation (RSD) of the PDD, $\sigma_r(\Delta^2\phi)$, is sufficiently large,

$$\sigma_r(\Delta^2\phi) > \frac{k|\delta\Gamma_E|T^2}{\Delta^2\phi} \left\{ \sum_{j=1,2} \sum_{I=C,F} [\sigma^2(z_{jI}) + T^2\sigma^2(v_{z_{jI}})] \right\}^{1/2}, \quad (4)$$

where $\sigma(z_{jI})$ and $\sigma(v_{z_{jI}})$ are the standard deviations (SD) of the initial atomic position and velocity. Although, starting with article [11], methods for measuring the gravity gradient using AIs have been studied in many articles, I know only three publications [14–16], in which the values of Γ_{E33} and $\delta\Gamma_{E33}$ were published. The error $\delta\Gamma_{E33} = 10E$ was reported [16]. For the values obtained in [3, 4], $\sigma(z_{jI}) \sim 10^{-4}\text{m}$, $\sigma(v_{z_{jI}}) \sim 3 \cdot 10^{-3}\text{m/s}$, $k \approx 1.61 \cdot 10^7\text{m}^{-1}$,

$$\Delta_s^2\phi = 0.547870(63)\text{rad}, \quad (5)$$

one gets

$$\sigma_r(\Delta^2\phi) > 7\text{ppm}. \quad (6)$$

We will make sure that the restriction (6) can be neglected with an accuracy of no more than 10%.

In order to achieve the maximum value of the first order difference $\Delta\phi_s^{(C)}$ in C -configuration, one can choose starting points at the maximum and minimum of the dependence $\phi_s^{(C)}(z, v)$ [5, 10]. The choice of extreme points leads to a quadratic dependence of the phase $\phi_s^{(C)}(z, v)$ on small deviations $\{\delta z_j, \delta v_j\}$ in the vicinities of these points.

Let us consider now the contribution to the phase double difference from the first-order phase difference in F -configuration. In principle, one can find the positions of the halves of the source mass, at which points z_1 and z_2 are extrema of the dependence $\phi_s^{(F)}(z, v)$ [18]. However, in this case, points in the velocity space v_{z_1} and v_{z_2} , which were extreme for the C -configuration, become non-extreme. To avoid this difficulty one can [5, 10] distance the halves of the source mass sufficiently far so that even the linear dependences of the $\phi_s^{(F)}(z, v)$ on the deviations near the points $\{z_j, v_j\}$ do not affect significantly the error $\phi_s^{(C)}$ of the phase double differences (2).

We performed [5, 10] calculations, determined the optimal geometry of the gravitational field, positions and velocities of atomic clouds for the source mass of a cuboid shape. The choice of this shape is convenient for calculations since one has an analytical expression for the potential of the cuboid [19]. Despite this, it is preferable to use the source mass in a cylindrical shape to perform high-precision measurements of G [20]. Cylindrical source masses were used to measure G with an accuracy of 150ppm [3, 4]. The hollow cylinder source mass has been proposed to achieve an accuracy of 10ppm [13]. The analytical expression for the gravitational field along the axis of the hollow cylinder was explored [13], but outside this axis, the potential expansion into spherical harmonics was used [3, 4]. The technique for calculating the gravitational field without calculating the gravitational potential was proposed in book [20], but the final expression for the cylinder field is given in [20] without derivation. Following technique [20], we calculated the field and arrived at expressions (A17, A22) that do not coincide with those given in [20]. Both the derivations and final results are presented in this article.

To estimate the expected accuracy of the G -measurement, one has to analyze the error $\phi_s^{(C)}$. In precision gravity experiments, one calculates or measures the SD σ of the response f (such as the AI phase or phase difference) using the expression

$$\sigma(f) = \left(\sum_{m=1}^n \sigma_m^2 \right)^{1/2}, \quad (7)$$

where n is the number of variables $\{q_1, \dots, q_n\}$, included in the error budget, $\sigma_m = |\partial f / \partial q_m| \sigma(q_m)$, and $\sigma(q_m)$ is a SD of small uncertainty in the variable q_m . See examples of such budgets in [2–4, 13, 14, 18, 21]. The situation changes when one considers uncertainties near the extreme points $\{\mathbf{x}_m, \mathbf{v}_m\}$ and the signal uncertainty becomes a quadratic function of the uncertainties of the atomic position and velocity $\{\delta\mathbf{x}_m, \delta\mathbf{v}_m\}$. There are several examples in which measurements were carried out (or proposed to be carried out) near extreme points. Extreme atomic coordinates were selected in the experiments [18]. Extreme atomic coordinates and velocities were found in the articles [5, 10]. The difficulties of using extreme points are noted in the article [13], where an alternative approach was proposed,

based on the elimination of the dependence of the AI phase on the atomic position and velocity proposed in [12]. However, even in this case, one eliminates only the dependence on the vertical coordinates and velocities, while the transverse coordinates $\{x_m, y_m\} = \{0, 0\}$ and velocities $\{v_{x_m}, v_{y_m}\} = \{0, 0\}$ remain extreme. This is because the vertical component of the gravitational field of the hollow cylinder $\delta g_z(\mathbf{x})$ is axially symmetric, and the expansion of both the field and the field gradient in transverse coordinates begins with quadratic terms. We see that in all the cases listed above [5, 10, 13, 18], the use of the expression (7) is unjustified. Revision of this expression is required. Moreover, the quadratic dependence on the uncertainties $\{\delta \mathbf{x}_m, \delta \mathbf{v}_m\}$ leads to a shift in the signal [22]. Here, we expressed both the SD and the shift of the phase double difference (2) in terms of the first and second derivatives of the phases $\phi_s^{(C,F)}$ at the found extreme points.

The article is arranged as follows. Standard deviation and shift are obtained in the next section. Section III is devoted to the AI phase and phase derivatives calculations, PDD and error budget for source mass consisting of 24 cylinders are obtained in the Sec. IV. An optimization procedure in respect to atomic positions and velocities considered in the Sec. V. The case of the 630 cylinders source mass is studied in the Sec. VI, while the derivation of the cylinder gravitational field is presented in the Appendix.

II. SD AND SHIFT.

Let us consider the variation of the double difference (2)

$$\begin{aligned} \delta \Delta^{(2)} \phi & [\delta \mathbf{x}_{1C}, \delta \mathbf{v}_{1C}, \delta \mathbf{x}_{2C}, \delta \mathbf{v}_{2C}; \delta \mathbf{x}_{1F}, \delta \mathbf{v}_{1F}, \delta \mathbf{x}_{2F}, \delta \mathbf{v}_{2F}] \\ & = \delta \phi^{(C)} [\delta \mathbf{x}_{1C}, \delta \mathbf{v}_{1C}] - \delta \phi^{(C)} [\delta \mathbf{x}_{2C}, \delta \mathbf{v}_{2C}] \\ & - [\delta \phi^{(F)} (\delta \mathbf{x}_{1F}, \delta \mathbf{v}_{1F}) - \delta \phi^{(F)} (\delta \mathbf{x}_{2F}, \delta \mathbf{v}_{2F})], \end{aligned} \quad (8)$$

where $\{\delta \mathbf{x}_{jI}, \delta \mathbf{v}_{jI}\}$ is the uncertainty of the launching position and velocity of the cloud j ($j = 1$ or 2) for the source mass configuration I ($I = C$ or F), $\delta \phi^{(I)} (\delta \mathbf{x}_{jI}, \delta \mathbf{v}_{jI})$ is the variation of the AI j phase, produced when the source mass gravity field is in the I -configuration. For the shift s and standard deviation σ defined as

$$s (\Delta^{(2)} \phi) = \left\langle \delta \Delta^{(2)} \phi [\delta \mathbf{x}_{1C}, \delta \mathbf{v}_{1C}, \delta \mathbf{x}_{2C}, \delta \mathbf{v}_{2C}; \delta \mathbf{x}_{1F}, \delta \mathbf{v}_{1F}, \delta \mathbf{x}_{2F}, \delta \mathbf{v}_{2F}] \right\rangle, \quad (9a)$$

$$\sigma (\Delta^{(2)} \phi) = \left\{ \left\langle [\delta \Delta^{(2)} \phi (\delta \mathbf{x}_{1C}, \delta \mathbf{v}_{1C}, \delta \mathbf{x}_{2C}, \delta \mathbf{v}_{2C}; \delta \mathbf{x}_{1F}, \delta \mathbf{v}_{1F}, \delta \mathbf{x}_{2F}, \delta \mathbf{v}_{2F})]^2 \right\rangle - s^2 (\Delta^{(2)} \phi) \right\}^{1/2} \quad (9b)$$

one finds

$$s (\Delta^{(2)} \phi) = s [\phi^{(C)} (\delta \mathbf{x}_{1C}, \delta \mathbf{v}_{1C})] - s [\phi^{(C)} (\delta \mathbf{x}_{2C}, \delta \mathbf{v}_{2C})] - s [\phi^{(F)} (\delta \mathbf{x}_{1F}, \delta \mathbf{v}_{1F})] + s [\phi^{(F)} (\delta \mathbf{x}_{2F}, \delta \mathbf{v}_{2F})], \quad (10a)$$

$$\sigma (\Delta^{(2)} \phi) = \left\{ \sum_{I=C,F} \sum_{j=1,2} \sigma^2 [\phi^{(I)} (\delta \mathbf{x}_{jI}, \delta \mathbf{v}_{jI})] \right\}^{1/2}, \quad (10b)$$

$$s [\phi^{(I)} (\delta \mathbf{x}_{jI}, \delta \mathbf{v}_{jI})] = \left\langle \delta \phi^{(I)} (\delta \mathbf{x}_{jI}, \delta \mathbf{v}_{jI}) \right\rangle \quad (10c)$$

$$\sigma [\phi^{(I)} (\delta \mathbf{x}_{jI}, \delta \mathbf{v}_{jI})] = \left\{ \left\langle [\delta \phi^{(I)} (\delta \mathbf{x}_{jI}, \delta \mathbf{v}_{jI})]^2 \right\rangle - \left\langle \delta \phi^{(I)} (\delta \mathbf{x}_{jI}, \delta \mathbf{v}_{jI}) \right\rangle^2 \right\}^{1/2} \quad (10d)$$

One sees that the problem is reduced to the calculation of the shift s and SD σ of a variation $\delta \phi [\delta \mathbf{x}, \delta \mathbf{v}]$. The phase of the given AI at the given configuration of the source mass comprises two parts

$$\phi (\mathbf{x}, \mathbf{v}) = \phi_E (\mathbf{x}, \mathbf{v}) + \phi_s (\mathbf{x}, \mathbf{v}), \quad (11)$$

where for the phase induced by the Earth's field, under some simplifying assumptions (see, for example, [23]), one gets

$$\phi_E^{(I)} (\mathbf{x}_j, \mathbf{v}_j) = \mathbf{k} \cdot \mathbf{g} T^2 + \mathbf{k} \cdot \Gamma_E T^2 (\mathbf{x} + \mathbf{v} T) + \mathbf{k} \cdot \Gamma_E \mathbf{g} T^2 \left(\frac{7}{12} T^2 + T T_1 + \frac{1}{2} T_1^2 \right), \quad (12)$$

where T_1 is the time delay between the moment the atoms are launched and the 1st Raman pulse. For the vertical wave vector $\mathbf{k} = (0, 0, k)$, expanding Eq. (11).to the second order terms one gets

$$\delta\phi(\delta\mathbf{x}, \delta\mathbf{v}) = \left(\tilde{\gamma}_{xm} + \frac{\partial\phi_s}{\partial x_m}\right)\delta x_m + \left(\tilde{\gamma}_{vm} + \frac{\partial\phi_s}{\partial v_m}\right)\delta v_m + \frac{1}{2}\frac{\partial^2\phi_s}{\partial x_m\partial x_n}\delta x_m\delta x_n + \frac{1}{2}\frac{\partial^2\phi_s}{\partial v_m\partial v_n}\delta v_m\delta v_n + \frac{\partial^2\phi_s}{\partial x_m\partial v_n}\delta x_m\delta v_n, \quad (13)$$

where

$$\tilde{\gamma}_{xm} = k\Gamma_{E3m}T^2; \quad (14a)$$

$$\tilde{\gamma}_{vm} = T\tilde{\gamma}_{xm} \quad (14b)$$

A summation convention implicit in Eq. (13) will be used in all subsequent equations. Repeated indices and symbols appearing on the right-hand-side (rhs) of an equation are to be summed over, unless they also appear on the left-hand-side (lhs) of that equation. Let assume that the distribution functions of the uncertainties are sufficiently symmetric, and all odd moments are equal 0. The moments of the second and fourth orders are given by

$$\langle\delta x_m\delta x_n\rangle = \delta_{mn}\sigma^2(x_m), \quad (15a)$$

$$\begin{aligned} \langle\delta x_m\delta x_n\delta x_{m'}\delta x_{n'}\rangle = & \delta_{mn}\delta_{m'n'}\sigma^2(x_m)\sigma^2(x_{m'}) + (\delta_{mm'}\delta_{nn'} + \delta_{mn'}\delta_{nm'})\sigma^2(x_m)\sigma^2(x_n) \\ & + \delta_{mn}\delta_{mm'}\delta_{mn'}\kappa(x_m)\sigma^4(x_m), \end{aligned} \quad (15b)$$

where δ_{mn} is Kronecker symbol, $\kappa(x_m)$ is a cumulant of the given uncertainty δx_m , defined as

$$\kappa(x_m) = \frac{\langle\delta x_m^4\rangle}{\sigma^4(x_m)} - 3. \quad (16)$$

Using the moments (15) one arrives at the following expressions for the SD and shift

$$\begin{aligned} \sigma[\phi(\delta\mathbf{x}, \delta\mathbf{v})] = & \left\{ \left(\tilde{\gamma}_{xm} + \frac{\partial\phi_s}{\partial x_m}\right)^2\sigma^2(x_m) + \left(\tilde{\gamma}_{vm} + \frac{\partial\phi_s}{\partial v_m}\right)^2\sigma^2(v_m) \right. \\ & + \frac{1}{2}\left[\left(\frac{\partial^2\phi}{\partial x_m\partial x_n}\right)^2\sigma^2(x_m)\sigma^2(x_n) + \left(\frac{\partial^2\phi}{\partial v_m\partial v_n}\right)^2\sigma^2(v_m)\sigma^2(v_n)\right] \\ & \left. + \left(\frac{\partial^2\phi}{\partial x_m\partial v_n}\right)^2\sigma^2(x_m)\sigma^2(v_n) + \frac{1}{4}\left[\left(\frac{\partial^2\phi}{\partial x_m^2}\right)^2\kappa(x_m)\sigma^4(x_m) + \left(\frac{\partial^2\phi}{\partial v_m^2}\right)^2\kappa(v_m)\sigma^4(v_m)\right]\right\}^{1/2} \end{aligned} \quad (17a)$$

$$s[\phi(\delta\mathbf{x}, \delta\mathbf{v})] = \frac{1}{2}\left(\frac{\partial^2\phi}{\partial x_m^2}\sigma^2(x_m) + \frac{\partial^2\phi}{\partial v_m^2}\sigma^2(v_m)\right), \quad (17b)$$

One sees that, even for the symmetric uncertainties distribution, the knowledge of the uncertainties' SDs is not sufficient. One has to know also uncertainties' cumulants (16). The exclusion here is Gaussian distributions, for which the cumulants

$$\kappa(x_m) = \kappa(v_m) = 0. \quad (18)$$

Further calculations will be performed only for these distributions.

For the each case considered below we are going to calculate the double difference (2) and relative contributions to the shift (9a) and SD (9b) from the each of two atom clouds at the each of two source mass configurations.

III. THE PHASE AND PHASE DERIVATIVES OF THE ATOM INTERFEROMETER

To calculate the phase $\phi_s^{(I)}$ produced by the gravitational field of the source mass, we use the results obtained in the article [24]. It is necessary to distinguish three contributions to the phase, classical, quantum, and Q-term (see Eqs. (62c, 64, 60c), (62d, 71, 60c), (89) in [24] for these three terms). For Q-term an estimate was obtained

$$\frac{\phi_Q}{\phi_s^{(I)}} \sim \frac{1}{24}\left(\frac{\hbar kT}{LM_a}\right)^2, \quad (19)$$

where M_a is the atom mass, L is the characteristic distance over which the gravitational potential of the test mass changes. For ^{87}Rb , at $L > 0.3\text{m}$, the relative weight of the Q-term does not exceed 2ppb, and we neglect it. For the remaining terms and the vertical effective wave vector, $\mathbf{k} = \{0, 0, k\}$, one gets

$$\begin{aligned}\phi_s^{(I)}(\mathbf{x}, \mathbf{v}) = k \int_0^T dt \left\{ (T-t) \delta g_z \left[\mathbf{x} + \mathbf{v} (T_1 + T + t) + \frac{1}{2} \mathbf{g} (T_1 + T + t)^2 + \frac{\hbar \mathbf{k}}{2M} (T + t) \right] \right. \\ \left. + t \delta g_z \left[\mathbf{x} + \mathbf{v} (T_1 + t) + \frac{1}{2} \mathbf{g} (T_1 + t)^2 + \frac{\hbar \mathbf{k}}{2M} t \right] \right\},\end{aligned}\quad (20)$$

where $\delta g_z(\mathbf{x})$ is the vertical component of the gravitational field of the source mass. The derivatives of this phase of the first and second order are given by

$$\begin{aligned}\frac{\partial \phi_s^{(I)}(\mathbf{x}, \mathbf{v})}{\partial x_m} = k \int_0^T dt \left\{ (T-t) \gamma_{zm} \left[\mathbf{x} + \mathbf{v} (T_1 + T + t) + \frac{1}{2} \mathbf{g} (T_1 + T + t)^2 + \frac{\hbar \mathbf{k}}{2M} (T + t) \right] \right. \\ \left. + t \gamma_{zm} \left[\mathbf{x} + \mathbf{v} (T_1 + t) + \frac{1}{2} \mathbf{g} (T_1 + t)^2 + \frac{\hbar \mathbf{k}}{2M} t \right] \right\},\end{aligned}\quad (21a)$$

$$\begin{aligned}\frac{\partial \phi_s^{(I)}(\mathbf{x}, \mathbf{v})}{\partial v_m} = k \int_0^T dt \left\{ (T-t) (T_1 + T + t) \gamma_{zm} \left[\mathbf{x} + \mathbf{v} (T_1 + T + t) + \frac{1}{2} \mathbf{g} (T_1 + T + t)^2 + \frac{\hbar \mathbf{k}}{2M} (T + t) \right] \right. \\ \left. + t (T_1 + t) \gamma_{zm} \left[\mathbf{x} + \mathbf{v} (T_1 + t) + \frac{1}{2} \mathbf{g} (T_1 + t)^2 + \frac{\hbar \mathbf{k}}{2M} t \right] \right\},\end{aligned}\quad (21b)$$

$$\begin{aligned}\frac{\partial^2 \phi_s^{(I)}(\mathbf{x}, \mathbf{v})}{\partial x_m \partial x_n} = k \int_0^T dt \left\{ (T-t) \chi_{zmn} \left[\mathbf{x} + \mathbf{v} (T_1 + T + t) + \frac{1}{2} \mathbf{g} (T_1 + T + t)^2 + \frac{\hbar \mathbf{k}}{2M} (T + t) \right] \right. \\ \left. + t \chi_{zmn} \left[\mathbf{x} + \mathbf{v} (T_1 + t) + \frac{1}{2} \mathbf{g} (T_1 + t)^2 + \frac{\hbar \mathbf{k}}{2M} t \right] \right\},\end{aligned}\quad (21c)$$

$$\begin{aligned}\frac{\partial^2 \phi_s^{(I)}(\mathbf{x}, \mathbf{v})}{\partial x_m \partial v_n} = k \int_0^T dt \left\{ (T-t) (T_1 + T + t) \chi_{zmn} \left[\mathbf{x} + \mathbf{v} (T_1 + T + t) + \frac{1}{2} \mathbf{g} (T_1 + T + t)^2 + \frac{\hbar \mathbf{k}}{2M} (T + t) \right] \right. \\ \left. + t (T_1 + t) \chi_{zmn} \left[\mathbf{x} + \mathbf{v} (T_1 + t) + \frac{1}{2} \mathbf{g} (T_1 + t)^2 + \frac{\hbar \mathbf{k}}{2M} t \right] \right\},\end{aligned}\quad (21d)$$

$$\begin{aligned}\frac{\partial^2 \phi_s^{(I)}(\mathbf{x}, \mathbf{v})}{\partial v_m \partial v_n} = k \int_0^T dt \left\{ (T-t) (T_1 + T + t)^2 \chi_{zmn} \left[\mathbf{x} + \mathbf{v} (T_1 + T + t) + \frac{1}{2} \mathbf{g} (T_1 + T + t)^2 + \frac{\hbar \mathbf{k}}{2M} (T + t) \right] \right. \\ \left. + t (T_1 + t)^2 \chi_{zmn} \left[\mathbf{x} + \mathbf{v} (T_1 + t) + \frac{1}{2} \mathbf{g} (T_1 + t)^2 + \frac{\hbar \mathbf{k}}{2M} t \right] \right\},\end{aligned}\quad (21e)$$

where $\gamma_{zm}(\mathbf{x}) = \frac{\partial \delta g_z(\mathbf{x})}{\partial x_m}$ is the zm -component of the gravity-gradient tensor of the source mass field, and

$$\chi_{zmn}(\mathbf{x}) = \frac{\partial^2 \delta g_z(\mathbf{x})}{\partial x_m \partial x_n}\quad (22)$$

is the zmn -component of the curvature tensor of this field.

IV. ERROR BUDGET

We applied the formula for the cylinder field (A17) to calculate the phases produced by different sets of cylinders. In this section, we consider the field geometry chosen in the article [3, 4], see Fig. 1.

Two halves of the source mass, each including 12 tungsten alloy cylinders, move in a vertical direction from C -configuration to F -configuration, in each of which one measures the phase difference of the first order (1), and then PDD (2). The following system parameters are important for calculation: cylinder density $\rho = 18263\text{kg/m}^3$, cylinder radius and height $R = 0.0495\text{m}$ and $h = 0.15011\text{m}$, Newtonian gravitational constant $G = 6.67408 \cdot 10^{-11}\text{kg}^{-1}\text{m}^3\text{s}^{-2}$ [25], the Earth's gravitational field $g = 9.80492\text{m/s}^2$ [26], the delay between impulses $T = 160\text{ms}$, the time $T_1 = 0$, the effective wave vector $k = 1.61058 \cdot 10^7\text{m}^{-1}$, the mass of the ^{87}Rb $M = 86.9092\text{a.u.}$ [27], atomic velocity at the moment of the first impulse action $v = 1.62762\text{m/s}$. With respect to the apogee of the atomic trajectory in the lower interferometer, the z -coordinates of the centers of the halves of the source mass are equal to 0.04m and 0.261m in the

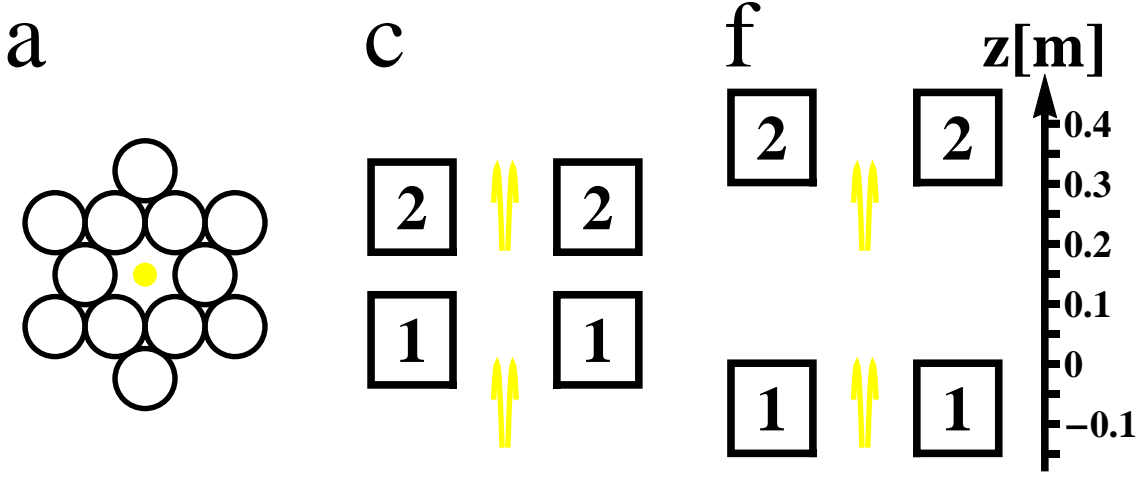


FIG. 1: The mutual positioning of the source mass halves 1 and 2, and atomic clouds. Top view (a), cross-sections $x=0$ for C-configuration (c) and F-configuration (f). Trajectories of atoms are shown in yellow.

TABLE I: Relative contributions to PDD and error budget for two configurations of source mass.

Term	C-configuration	F-configuration
$\pm \Delta_s \phi^I / \Delta^2 \phi$	0.685376	0.314624
Linear in position	$0.322\delta z_{1C} + 0.117\delta z_{2C} + 7.77 \cdot 10^5 \times [\Gamma_{E31}(\delta x_{1C} - \delta x_{2C}) + \Gamma_{E32}(\delta y_{1C} - \delta y_{2C})]$	$0.132\delta z_{1F} + 0.518\delta z_{2F} - 7.77 \cdot 10^5 \times [\Gamma_{E31}(\delta x_{1F} - \delta x_{2F}) + \Gamma_{E32}(\delta y_{1F} - \delta y_{2F})]$
Linear in velocity	$0.0377\delta v_{z1C} + 0.0150\delta v_{z2C} + 1.24 \cdot 10^5 \times [\Gamma_{E31}(\delta v_{x1C} - \delta v_{x2C}) + \Gamma_{E32}(\delta v_{y1C} - \delta v_{y2C})]$	$0.0132\delta v_{z1F} + 0.0683\delta v_{z2F} - 1.24 \cdot 10^5 \times [\Gamma_{E31}(\delta v_{x1F} - \delta v_{x2F}) + \Gamma_{E32}(\delta v_{y1F} - \delta v_{y2F})]$
Nonlinear in position	$12.3(\delta x_{1C}^2 + \delta y_{1C}^2) - 24.7\delta z_{1C}^2 + 12.2(\delta x_{2C}^2 + \delta y_{2C}^2) - 24.3\delta z_{2C}^2$	$15.5(\delta x_{1F}^2 + \delta y_{1F}^2) - 30.9\delta z_{1F}^2 + 15.7(\delta x_{2F}^2 + \delta y_{2F}^2) - 31.3\delta z_{2F}^2$
Nonlinear in velocity	$0.375(\delta v_{x1C}^2 + \delta v_{y1C}^2) - 0.750\delta v_{z1C}^2 + 0.351(\delta v_{x2C}^2 + \delta v_{y2C}^2) - 0.702\delta v_{z2C}^2$	$0.451(\delta v_{x1F}^2 + \delta v_{y1F}^2) - 0.901\delta v_{z1F}^2 + 0.468(\delta v_{x2F}^2 + \delta v_{y2F}^2) - 0.937\delta v_{z2F}^2$
Position-velocity cross term	$3.99(\delta v_{x1C}\delta x_{1C} + \delta v_{y1C}\delta y_{1C}) - 7.97\delta v_{z1C}\delta z_{1C} + 4.05(\delta v_{x2C}\delta x_{2C} + \delta v_{y2C}\delta y_{2C}) - 8.10\delta v_{z2C}\delta z_{2C}$	$5.10(\delta v_{x1F}\delta x_{1F} + \delta v_{y1F}\delta y_{1F}) - 10.2\delta v_{z1F}\delta z_{1F} + 5.08(\delta v_{x2F}\delta x_{2F} + \delta v_{y2F}\delta y_{2F}) - 10.2\delta v_{z2F}\delta z_{2F}$

C -configuration and $-0.074m$ and $0.377m$ in the F -configuration, z -coordinate of the atomic trajectory apogee in the upper interferometer is equal to $0.328m$ (see Fig. 1c,f). Using Eq. (20) we got for PDD

$$\Delta^2 \phi = 0.530535 \text{ rad}, \quad (23)$$

which is less than the value (5) obtained in the article [3, 4], by 3.2%. The difference seems to be related to the fact that in these calculations, the contributions from platforms and other sources of gravity were not taken into account. Table I contains relative contributions to the PDD from two configurations, besides the phase values, linear and quadratic terms in the relative phase variations, due to the uncertainties of atomic coordinates and velocities, obtained using Eqs. (13, 14, 21), are also given. We used the value of the zz -component of the gravity gradient tensor of the Earth field, $\Gamma_{E33} = 3.11 \cdot 10^{-6} \text{ s}^{-2}$, measured in the article [16]

Using these data and Eqs. (10a, 10b, 17, 18), one gets for the RSD and shift

$$\begin{aligned}
\sigma \left(\Delta_s^{(2)} \phi \right) = & \{ 0.104 \sigma^2 (z_{1C}) + 0.0137 \sigma^2 (z_{2C}) + 1.42 \cdot 10^{-3} \sigma^2 (v_{z1C}) + 2.24 \cdot 10^{-4} \sigma^2 (v_{z2C}) \\
& + 0.0173 \sigma^2 (z_{1F}) + 0.269 \sigma^2 (z_{2F}) + 1.75 \cdot 10^{-4} \sigma^2 (v_{z1F}) + 4.66 \cdot 10^{-3} \sigma^2 (v_{z2F}) \\
& + \sum_{j=1,2} \sum_{I=C,F} [6.04 \cdot 10^{11} (\Gamma_{E31}^2 \sigma^2 (x_{jI}) + \Gamma_{E32}^2 \sigma^2 (y_{jI})) + 1.55 \cdot 10^{10} (\Gamma_{E31}^2 \sigma^2 (v_{xjI}) + \Gamma_{E32}^2 \sigma^2 (v_{yjI}))] \\
& + 305 [\sigma^4 (x_{1C}) + \sigma^4 (y_{1C})] + 1220 \sigma^4 (z_{1C}) + 296 [\sigma^4 (x_{2C}) + \sigma^4 (y_{2C})] + 1180 \sigma^4 (z_{2C}) \\
& + 0.282 [\sigma^4 (v_{x1C}) + \sigma^4 (v_{y1C})] + 1.13 \sigma^4 (v_{z1C}) + 0.247 [\sigma^4 (v_{x2C}) + \sigma^4 (v_{y2C})] + 0.987 \sigma^4 (v_{z2C}) \\
& + 15.9 [\sigma^2 (x_{1C}) \sigma^2 (v_{x1C}) + \sigma^2 (y_{1C}) \sigma^2 (v_{y1C})] + 63.5 \sigma^2 (z_{1C}) \sigma^2 (v_{z1C}) \\
& + 16.4 [\sigma^2 (x_{2C}) \sigma^2 (v_{x2C}) + \sigma^2 (y_{2C}) \sigma^2 (v_{y2C})] + 65.6 \sigma^2 (z_{2C}) \sigma^2 (v_{z2C}) \\
& + 478 [\sigma^4 (x_{1F}) + \sigma^4 (y_{1F})] + 1910 \sigma^4 (z_{1F}) + 490 [\sigma^4 (x_{2F}) + \sigma^4 (y_{2F})] + 1960 \sigma^4 (z_{2F}) + \\
& + 0.406 [\sigma^4 (v_{x1F}) + \sigma^4 (v_{y1F})] + 1.63 \sigma^4 (v_{z1F}) + 0.439 [\sigma^4 (v_{x2F}) + \sigma^4 (v_{y2F})] + 1.76 \sigma^4 (v_{z2F}) \\
& + 26.0 [\sigma^2 (x_{1F}) \sigma^2 (v_{x1F}) + \sigma^2 (y_{1F}) \sigma^2 (v_{y1F})] + 104 \sigma^2 (z_{1F}) \sigma^2 (v_{z1F}) \\
& + 25.8 [\sigma^2 (x_{2F}) \sigma^2 (v_{x2F}) + \sigma^2 (y_{2F}) \sigma^2 (v_{y2F})] + 103 \sigma^2 (z_{2F}) \sigma^2 (v_{z2F}) \}^{1/2},
\end{aligned} \tag{24a}$$

$$\begin{aligned}
s \left(\Delta_s^{(2)} \phi \right) = & 12.3 [\sigma^2 (x_{1C}) + \sigma^2 (y_{1C})] - 24.7 \sigma^2 (z_{1C}) + 12.2 [\sigma^2 (x_{2C}) + \sigma^2 (y_{2C})] - 24.3 \sigma^2 (v_{z2C}) \\
& + 0.375 [\sigma^2 (v_{x1C}) + \sigma^2 (v_{y1C})] - 0.750 \sigma^2 (v_{z1C}) + 0.351 [\sigma^2 (v_{x2C}) + \sigma^2 (v_{y2C})] - 0.702 \sigma^2 (v_{z2C}) \\
& + 15.5 [\sigma^2 (x_{1F}) + \sigma^2 (y_{1F})] - 30.9 \sigma^2 (z_{1F}) + 15.7 [\sigma^2 (x_{2F}) + \sigma^2 (y_{2F})] - 31.3 \sigma^2 (z_{2F}) \\
& + 0.451 [\sigma^2 (v_{x1F}) + \sigma^2 (v_{y1F})] - 0.901 \sigma^2 (v_{z1F}) + 0.468 [\sigma^2 (v_{x2F}) + \sigma^2 (v_{y2F})] - 0.937 \sigma^2 (v_{z2F}).
\end{aligned} \tag{24b}$$

For SDs achieved in [3, 4]

$$\sigma (x_{jI}) = \sigma (y_{jI}) = 10^{-3} \text{m}, \tag{25a}$$

$$\sigma (z_{jI}) = 10^{-4} \text{m}, \tag{25b}$$

$$\sigma (v_{xjI}) = \sigma (v_{yjI}) = 6 \cdot 10^{-3} \text{m/s}, \tag{25c}$$

$$\sigma (v_{zjI}) = 3 \cdot 10^{-3} \text{m/s}, \tag{25d}$$

one arrives to the RSD and the shift

$$\sigma \left(\delta \Delta_s^{(2)} \phi \right) = 275 \text{ppm} [1 + 6.14 \cdot 10^{13} (\Gamma_{E31}^2 + \Gamma_{E32}^2)]^{1/2}, \tag{26a}$$

$$s \left(\delta \Delta_s^{(2)} \phi \right) = 199 \text{ppm}. \tag{26b}$$

The non-diagonal matrix elements of the gradient tensor of the Earth's field consist of three contributions arising from the fact that the Geoid is not spherical, from the rotation of the Earth, and from the anomalous part of the field. The first two contributions were taken into account exactly [17], and they are 3 orders of magnitude smaller than the diagonal element Γ_{E33} . We have not been able to find any information about the anomalous part of the Earth's gravitational field. However, it is seen that the non-diagonal elements of the tensor can be neglected with an accuracy of not more than 10% if

$$\sqrt{\Gamma_{E31}^2 + \Gamma_{E32}^2} < 58.5E. \tag{27}$$

V. PHASE DOUBLE DIFFERENCE AND ERROR BUDGET AT OPTIMAL CONDITIONS

Let us apply now for the system of 24 cylinders the optimization procedure proposed in [5, 10]. It should be noted that this procedure can be implemented only if the technique of eliminating the gradient of the Earth's gravitational field [12] has been previously applied. According to [18] and unlike [3, 4] we have chosen for calculations in this section the distance between the lower and upper set of cylinders $dh = 0.05 \text{m}$. Our first task is to find the points of maximum and minimum (in the space of coordinates and velocities $\{z, v_z\}$) of the phase produced by the source mass field in

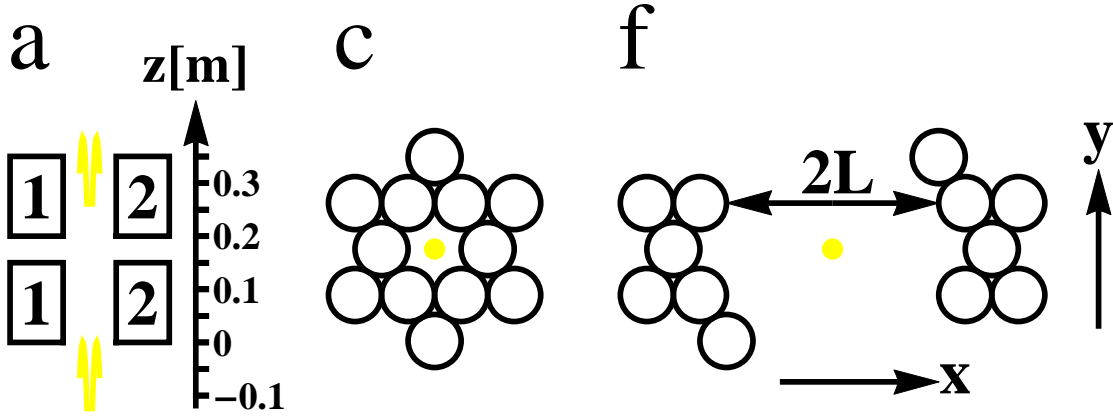


FIG. 2: The same as Fig. 1, but with different assignments for the halves 1 and 2. (a) The cross-section $y = 0$ for the C -configuration, (c) and (f), top views for C - and F -configurations.

TABLE II: The same as Table I, but at the optimal choice of the atomic positions and velocities in the C -configuration.

Term	C -configuration
Linear in position	$5.82 \cdot 10^{-5} \delta z_{1C} - 9.34 \cdot 10^{-7} \delta z_{2C}$
Linear in velocity	$1.30 \cdot 10^{-5} \delta v_{x1C} - 1.62 \cdot 10^{-7} \delta v_{z2C}$
Nonlinear in position	$-17.7 (\delta x_{1C}^2 + \delta y_{1C}^2) + 35.35 \delta z_{1C}^2 - 15.1 (\delta x_{2C}^2 + \delta y_{2C}^2) + 30.1 \delta z_{2C}^2$
Nonlinear in velocity	$-0.489 (\delta v_{x1C}^2 + \delta v_{y1C}^2) + 0.977 \delta v_{z1C}^2 - 0.451 (\delta v_{x2C}^2 + \delta v_{y2C}^2) + 0.902 \delta v_{z2C}^2$
Position-velocity cross term	$-5.66 (\delta v_{x1C} \delta x_{1C} + \delta v_{y1C} \delta y_{1C}) + 11.3 \delta v_{z1C} \delta z_{1C} - 4.82 (\delta v_{x2C} \delta x_{2C} + \delta v_{y2C} \delta y_{2C}) + 9.64 \delta v_{z2C} \delta z_{2C}$

C -configuration, $\phi_s^{(C)}$. Putting $T_1 = 0$, we found for these points (see Fig. 2)

$$\{z_{\max}, v_{\max}, \phi_s^{(C)}(z_{\max}, v_{z \max})\} = \{-0.124\text{m}, 1.56\text{m/s}, 0.215086\}, \quad (28a)$$

$$\{z_{\min}, v_{\min}, \phi_s^{(C)}(z_{\min}, v_{z \min})\} = \{0.261\text{m}, 1.56\text{m/s}, -0.212213\}. \quad (28b)$$

The velocities $v_{z \max}$ and $v_{z \min}$ coincide up to the fifth digit; up to the third digit, they coincide with the velocity of the atomic fountain [28] $v = gT = 1.569\text{m/s}$. The phase difference of the first order will be equal to

$$\Delta_s \phi^{(C)} = 0.427299\text{rad}. \quad (29)$$

At this stage, before performing the calculations in the F -configuration, we can calculate the shift and the RSD only with respect to the phase difference (29). Table II contains linear and quadratic terms in the relative variation of the phase $\Delta_s^{(C)}$, due to the uncertainties of atomic coordinates and velocities, obtained using Eqs. (13, 21)

One sees that despite the choice of extreme points, linear dependences in phase variation do not completely disappear. This is because extrema were found not exactly but approximately. If $\{z, v_z\}$ is a given approximate extreme point of the function $f(z, v_z)$, then using the iteration formulas

$$\{z, v_z\} \rightarrow \{z + \delta z, v_z + \delta v_z\}, \quad (30a)$$

$$\delta z = \left(\frac{\partial f}{\partial z} \frac{\partial^2 f}{\partial v_z^2} - \frac{\partial f}{\partial v_z} \frac{\partial^2 f}{\partial z^2} \right) \Big/ \left[\left(\frac{\partial^2 f}{\partial z \partial v_z} \right)^2 - \frac{\partial^2 f}{\partial z^2} \frac{\partial^2 f}{\partial v_z^2} \right], \quad (30b)$$

$$\delta v_z = \left(\frac{\partial f}{\partial v_z} \frac{\partial^2 f}{\partial z^2} - \frac{\partial f}{\partial z} \frac{\partial^2 f}{\partial v_z^2} \right) \Big/ \left[\left(\frac{\partial^2 f}{\partial z \partial v_z} \right)^2 - \frac{\partial^2 f}{\partial z^2} \frac{\partial^2 f}{\partial v_z^2} \right], \quad (30c)$$

one can find out the extremum with any arbitrarily high accuracy.

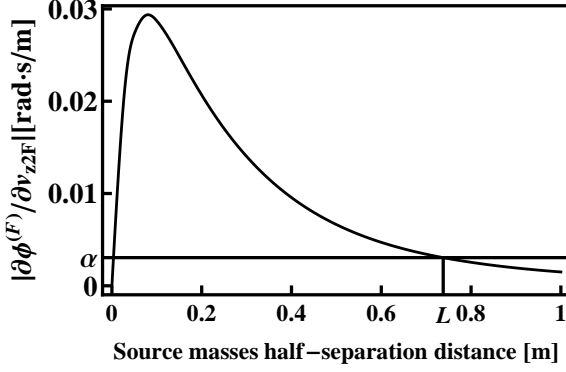


FIG. 3: To determine the distance L by which one should move the halves of the source mass in the F -configuration.

Using the data from Table II and Eqs. (10a, 10b, 17, 18), one gets for the RSD and relative shift

$$\begin{aligned} \sigma(\Delta_s^{(C)}\phi) = & \{625[\sigma^4(x_{1C}) + \sigma^4(y_{1C})] + 2500\sigma^4(z_{1C}) + 454[\sigma^4(x_{2C}) + \sigma^4(y_{2C})] + 1816\sigma^4(z_{2C}) \\ & + 0.477[\sigma^4(v_{x1C}) + \sigma^4(v_{y1C})] + 1.91\sigma^4(v_{z1C}) + 0.407[\sigma^4(v_{x2C}) + \sigma^4(v_{y2C})] \\ & + 1.63\sigma^4(v_{z2C}) + 32.0[\sigma^2(x_{1C})\sigma^2(v_{x1C}) + \sigma^2(y_{1C})\sigma^2(v_{y1C})] + 128\sigma^2(z_{1C})\sigma^2(v_{z1C}) \\ & + 23.2[\sigma^2(x_{2C})\sigma^2(v_{x2C}) + \sigma^2(y_{2C})\sigma^2(v_{y2C})] + 93.0\sigma^2(z_{2C})\sigma^2(v_{z2C})\}^{1/2}, \end{aligned} \quad (31a)$$

$$\begin{aligned} s(\Delta_s^{(C)}\phi) = & -17.7[\sigma^2(x_{1C}) + \sigma^2(y_{1C})] + 35.3\sigma^2(z_{1C}) - 15.1[\sigma^2(x_{2C}) + \sigma^2(y_{2C})] + 30.1\sigma^2(v_{z2C}) \\ & - 0.489[\sigma^2(v_{x1C}) + \sigma^2(v_{y1C})] + 0.977\sigma^2(v_{z1C}) - 0.451[\sigma^2(v_{x2C}) + \sigma^2(v_{y2C})] + 0.902\sigma^2(v_{z2C}). \end{aligned} \quad (31b)$$

At the uncertainties (25) one gets

$$\sigma(\Delta_s^{(C)}\phi) = 93\text{ppm}, \quad (32a)$$

$$s(\Delta_s^{(C)}\phi) = -116\text{ppm} \quad (32b)$$

Now consider the F -configuration. In this configuration, points $\{z_{1F}, v_{z1F}\} = \{z_{\max}, v_{\max}\}$ and $\{z_{2F}, v_{z2F}\} = \{z_{\min}, v_{\min}\}$ found above are not extreme, and therefore the main contribution to the variation of the phase difference of the first order, $\delta\Delta_s^{(F)}\phi$, arises from the linear terms. Including only these terms, one receives for RSD from Eqs. (10b, 17b)

$$\begin{aligned} \sigma(\Delta_s^{(F)}\phi) \approx & \left\{ \left[\frac{\partial\phi^{(F)}(z_{1F}, v_{z1F})}{\partial z_{1F}} \frac{\sigma(z_{1F})}{\Delta_s\phi^{(C)}} \right]^2 + \left[\frac{\partial\phi^{(F)}(z_{1F}, v_{z1F})}{\partial v_{z1F}} \frac{\sigma(v_{z1F})}{\Delta_s\phi^{(C)}} \right]^2 \right. \\ & \left. + \left[\frac{\partial\phi^{(F)}(z_{2F}, v_{z2F})}{\partial z_{2F}} \frac{\sigma(z_{2F})}{\Delta_s\phi^{(C)}} \right]^2 \sigma^2(z_{2F}) + \left[\frac{\partial\phi^{(F)}(z_{2F}, v_{z2F})}{\partial v_{z2F}} \frac{\sigma(v_{z2F})}{\Delta_s\phi^{(C)}} \right]^2 \right\}^{1/2} \end{aligned} \quad (33)$$

The distance $2L$ between the halves of the source mass should be chosen so large that an increase in RSD (32a) would be insignificant. Specifically, we demanded a full RSD did not exceed (32a) on the amount more than 10%, which means that

$$\sigma(\Delta_s^{(F)}\phi) \leq \sqrt{0.21}\sigma(\Delta_s^{(C)}\phi). \quad (34)$$

One can guarantee the fulfillment of this condition if the absolute value of the each of four terms in square brackets in (33) is less than $(\sqrt{0.21}/2)\sigma(\Delta_s^{(C)}\phi)$. The most dangerous here is the last term in (33). From the Fig. 3 one can be sure that the inequality

$$\left| \frac{\partial\phi^{(F)}(z_{2F}, v_{z2F})}{\partial v_{z2F}} \right| \leq \alpha, \quad (35)$$

TABLE III: The same as in Table I, but at the optimal choice of the atomic positions and velocities in the C -configuration, and after horizontal moving apart the halves of the source mass in the opposite directions by the distance (37) in the F -configuration.

Term	C -configuration	F -configuration
$\Delta_s^{(I)}\phi/\Delta_s^2\phi$	1.020272	-0.020272
Linear in position	$5.94 \cdot 10^{-5} \delta z_{1C} - 9.53 \cdot 10^{-7} \delta z_{2C}$	$[4.51 \delta z_{1F} - 4.55 \delta z_{2F}] \cdot 10^{-2}$
Linear in velocity	$1.33 \cdot 10^{-5} \delta v_{z1C} - 1.66 \cdot 10^{-7} \delta v_{z2C}$	$[7.21 \delta v_{z1F} - 7.28 \delta v_{z2F}] \cdot 10^{-3}$
Nonlinear in position	$-18.0 (\delta x_{1C}^2 + \delta y_{1C}^2) + 36.1 \delta z_{1C}^2$ $-15.4 (\delta x_{2C}^2 + \delta y_{2C}^2) + 30.7 \delta z_{2C}^2$	$[-72.6 \delta x_{1F}^2 + 19.2 \delta y_{1F}^2 + 53.4 \delta z_{1F}^2]$ $-9.93 \delta x_{1F} \delta v_{y1F}$ $-71.5 \delta x_{2F}^2 + 18.8 \delta y_{2F}^2 - 52.6 \delta z_{2F}^2$ $-9.78 \delta x_{2F} \delta y_{2F}] \cdot 10^{-3}$
Nonlinear in velocity	$-0.498 (\delta v_{x1C}^2 + \delta v_{y1C}^2)$ $+0.997 \delta v_{z1C}^2$ $-0.460 (\delta v_{x2C}^2 + \delta v_{y2C}^2)$ $+0.921 \delta v_{z2C}^2$	$[-21.9 \delta v_{x1F}^2 + 5.81 \delta v_{y1F}^2]$ $+16.1 \delta v_{z1F}^2 - 3.00 \delta v_{x1F} \delta v_{y1F}$ $-21.0 \delta v_{x2F}^2 + 5.52 \delta v_{y2F}^2$ $+15.5 \delta v_{z2F}^2 - 2.87 \delta v_{x2F} \delta v_{y2F}] \cdot 10^{-4}$
position-velocity cross term	$-5.77 (\delta v_{x1C} \delta x_{1C} + \delta v_{y1C} \delta y_{1C})$ $+11.5 \delta v_{z1C} \delta z_{1C}$ $-4.92 (\delta v_{x2C} \delta x_{2C} + \delta v_{y2C} \delta y_{2C})$ $+9.84 \delta v_{z2C} \delta z_{2C}$	$[-23.2 \delta v_{x1F} \delta x_{1F} + 6.13 \delta v_{y1F} \delta y_{1F}]$ $+17.1 \delta v_{z1F} \delta z_{1F} - 1.59 (\delta v_{y1F} \delta x_{1F} + \delta v_{x1F} \delta y_{1F})$ $-22.9 \delta v_{x2F} \delta x_{2F} + 6.02 \delta v_{y2F} \delta y_{2F} + 16.8 \delta v_{z2F} \delta z_{2F}$ $-1.56 (\delta v_{y2F} \delta x_{2F} + \delta v_{x2F} \delta y_{2F})] \cdot 10^{-3}$

where

$$\alpha = \frac{\sqrt{0.21} \Delta_s \phi^{(C)}}{2 \sigma(v_{z2F})} \sigma(\Delta_s^{(C)} \phi) = 3.05 \cdot 10^{-3}, \quad (36)$$

is satisfied starting from the value

$$L = 0.738 \text{m}. \quad (37)$$

After the halves of the source mass are moved apart by distances of $\pm L$, we get for the phase difference

$$\Delta_s^{(F)} \phi = 8.49006 \text{mrad}, \quad (38)$$

and therefore the PDD decreases to the value

$$\Delta^2 \phi = 0.418809. \quad (39)$$

Calculating [with the use of Eqs. (21)] derivatives of the interferometers' phases, one arrives to the relative contributions to the PDD presented in the Table III. With the data from this table one gets following final expressions for the RSD and shift

$$\begin{aligned}
\sigma \left(\Delta_s^{(2)} \phi \right) = & \{ 650. [\sigma^4(x_{1C}) + \sigma^4(y_{1C})] + 2600\sigma^4(z_{1C}) + 473 [\sigma^4(x_{2C}) + \sigma^4(y_{2C})] + 1890\sigma^4(z_{2C}) \\
& + 0.497 [\sigma^4(v_{x1C}) + \sigma^4(v_{y1C})] + 1.99\sigma^4(v_{z1C}) + 0.424 [\sigma^4(v_{x2C}) + \sigma^4(v_{y2C})] + 1.69\sigma^4(v_{z2C}) \\
& + 33.3 [\sigma^2(x_{1C})\sigma^2(v_{x1C}) + \sigma^2(y_{1C})\sigma^2(v_{y1C})] + 133\sigma^2(z_{1C})\sigma^2(v_{z1C}) \\
& + 24.2 [\sigma^2(x_{2C})\sigma^2(v_{x2C}) + \sigma^2(y_{2C})\sigma^2(v_{y2C})] + 96.8\sigma^2(z_{2C})\sigma^2(v_{z2C}) \\
& + [2.03\sigma^2(z_{1F}) + 2.07\sigma^2(z_{2F})] \cdot 10^{-3} + [5.20\sigma^2(v_{z1F}) + 5.30\sigma^2(v_{z2F})] \cdot 10^{-5} \\
& + [1050\sigma^4(x_{1F}) + 73.4\sigma^4(y_{1F}) + 9.85\sigma^2(x_{1F})\sigma^2(y_{1F}) + 570\sigma^4(z_{1F}) \\
& + 1020\sigma^4(x_{2F}) + 70.9\sigma^4(y_{2F}) + 9.56\sigma^2(x_{2F})\sigma^2(y_{2F}) + 554\sigma^4(z_{2F})] \cdot 10^{-5} \\
& + [963\sigma^4(v_{x1F}) + 67.5\sigma^4(v_{y1F}) + 9.00\sigma^2(v_{x1F})\sigma^2(v_{y1F}) + 520\sigma^4(v_{z1F}) \\
& + 881\sigma^4(v_{x2F}) + 60.9\sigma^4(v_{y2F}) + 8.25\sigma^2(v_{x2F})\sigma^2(v_{y2F}) + 479\sigma^4(v_{z2F})] \cdot 10^{-8} \\
& + [539\sigma^2(x_{1F})\sigma^2(v_{x1F}) + 2.52\sigma^2(x_{1F})\sigma^2(v_{y1F}) + 37.6\sigma^2(y_{1F})\sigma^2(v_{y1F}) \\
& + 292\sigma^2(z_{1F})\sigma^2(v_{z1F}) + 523\sigma^2(x_{2F})\sigma^2(v_{x2F}) + 36.3\sigma^2(y_{2F})\sigma^2(v_{y2F}) \\
& + 2.45\sigma^2(y_{2F})\sigma^2(v_{x2F}) + 284\sigma^2(z_{2F})\sigma^2(v_{z2F})] \cdot 10^{-6} \}^{1/2}, \tag{40a}
\end{aligned}$$

$$\begin{aligned}
s \left(\Delta_s^{(2)} \phi \right) = & -18.0 [\sigma^2(x_{1C}) + \sigma^2(y_{1C})] + 36.1\sigma^2(z_{1C}) - 15.4 [\sigma^2(x_{2C}) + \sigma^2(y_{2C})] + 30.74\sigma^2(v_{z2C}) \\
& - 0.498 [\sigma^2(v_{x1C}) + \sigma^2(v_{y1C})] + 0.997\sigma^2(v_{z1C}) - 0.460 [\sigma^2(v_{x2C}) + \sigma^2(v_{y2C})] + 0.921\sigma^2(v_{z2C}) \\
& [-726\sigma^2(x_{1F}) + 192\sigma^2(y_{1F}) + 534\sigma^2(z_{1F}) - 715\sigma^2(x_{2F}) + 188\sigma^2(y_{2F}) + 526\sigma^2(z_{2F}) - 21.9\sigma^2(v_{x1F}) \\
& + 5.81\sigma^2(v_{y1F}) + 16.1\sigma^2(v_{z1F}) - 21.0\sigma^2(v_{x2F}) + 5.52\sigma^2(v_{y2F}) + 15.5\sigma^2(v_{z2F})] \cdot 10^{-4} \tag{40b}
\end{aligned}$$

For the uncertainties (25) in the atomic positions and velocities, which we choose here following achievements in [3, 4], one gets

$$\sigma \left(\Delta_s^{(2)} \phi \right) = 100 \text{ ppm}, \tag{41a}$$

$$s \left(\Delta_s^{(2)} \phi \right) = 118 \text{ ppm}. \tag{41b}$$

In this section, we considered the movements of the halves of the source mass in the horizontal plane from the C -configuration to the F -configuration. Another option was considered in the article [13], in which it was assumed that the source mass as a whole moves in the vertical direction. To determine the distance L of the displacement in the vertical direction, it is necessary to return to the Eq. (33) and inequality (34). The calculation showed that in this case the greatest danger is again the last term in braces in the equation (33). So we return to inequality (35). Solving it numerically, one obtains that the displacement must be not less than

$$L = 1.33 \text{ m}. \tag{42}$$

Since this distance is 1.8 times greater than the distance (37), one concludes that horizontal displacement is preferable than vertical displacement. I would also like to emphasize that the horizontal displacement of the source mass was implemented in the article [9].

VI. 13 TONS SOURCE MASS

We have already mentioned above that G. Rosi proposed and studied [13] a new approach to the measurement of G with an accuracy of 10 ppm, based on the technique of eliminating the gravity-gradient terms [12]. In addition to the new technique, estimates have been performed for the source mass weight increased to the 13 tons, time separation between Raman pulses increased to

$$T = 243 \text{ ms}, \tag{43}$$

and the uncertainty of the velocity of atomic clouds reduced to

$$\sigma(v_{xjI}) = \sigma(v_{yjI}) = 2 \text{ mm/s}, \tag{44a}$$

$$\sigma(v_{zjI}) = 0.3 \text{ mm/s}. \tag{44b}$$

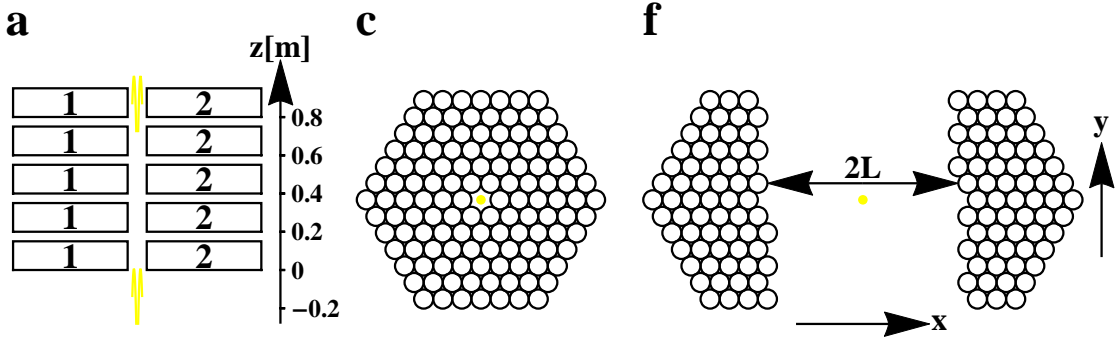


FIG. 4: Same as Fig. 2, but for 630 cylinders.

TABLE IV: The same as Table II, but for the 630 cylinders.

Term	C-configuration
Linear in position	$-9.25 \cdot 10^{-8} \delta z_{1C} + 1.28 \cdot 10^{-7} \delta z_{2C}$
Linear in velocity	$-1.79 \cdot 10^{-8} \delta v_{z1C} + 1.18 \cdot 10^{-7} \delta v_{z2C}$
Nonlinear in position	$4.92 (\delta x_{1C}^2 + \delta y_{1C}^2) - 9.84 \delta z_{1C}^2 + 2.97 (\delta x_{2C}^2 + \delta y_{2C}^2) - 5.95 \delta z_{2C}^2$
Nonlinear in velocity	$0.306 (\delta v_{x1C}^2 + \delta v_{y1C}^2) - 0.612 \delta v_{z1C}^2 + 0.197 (\delta v_{x2C}^2 + \delta v_{y2C}^2) - 0.393 \delta v_{z2C}^2$
Position-velocity cross term	$2.39 (\delta v_{x1C} \delta x_{1C} + \delta v_{y1C} \delta y_{1C}) - 4.78 \delta v_{z1C} \delta z_{1C} + 1.45 (\delta v_{x2C} \delta x_{2C} + \delta v_{y2C} \delta y_{2C}) - 2.89 \delta v_{z2C} \delta z_{2C}$

In this section we show that the optimization of PDD applied to set of cylinders used in [3, 4], with a total weight of about 13 tons and uncertainties of the atomic initial positions and velocities (25a, 25b) and (44), can also lead to accuracy of PDD measurement of the order of 10 ppm. Specifically, we assume that the cylinders are located on a 5-storey structure with a distance between the floors of 0.20011m. Each of the floors has 126 cylinders as shown in Fig. 4c,f. This arrangement of the cylinders is a natural generalization of the geometry chosen in the [3, 4].

Maximum and minimum points of the function $\phi^{(C)}(z, v)$,

$$\{z_{\max}, v_{z \max}, \phi_s^{(C)}(z_{\max}, v_{z \max})\} = \{-0.281\text{m}, 2.38\text{m/s}, 1.84859\text{rad}\}, \quad (45\text{a})$$

$$\{z_{\min}, v_{z \min}, \phi_s^{(C)}(z_{\min}, v_{z \min})\} = \{0.727\text{m}, 2.38\text{m/s}, -1.81252\text{rad}\}, \quad (45\text{b})$$

one selects for the initial coordinates and velocities of the atomic clouds in the first and second interferometer. The phase difference of the first order in this case is

$$\Delta_s^{(C)} \phi = 3.66111\text{rad}. \quad (46)$$

Linear and quadratic terms in relative variations $\delta \Delta_s^{(C)} \phi / \Delta_s^{(C)} \phi$ are pieced together in the Table IV. Substituting these data into the equations (17), one obtains for RSD and shift

$$\begin{aligned} \sigma(\Delta_s^{(C)} \phi) = & \{48.4 [\sigma^4(x_{1C}) + \sigma^4(y_{1C})] + 194\sigma^4(z_{1C}) + 17.7 [\sigma^4(x_{2C}) + \sigma^4(y_{2C})] + 70.8\sigma^4(z_{2C}) \\ & + 0.187 [\sigma^4(v_{x1C}) + \sigma^4(v_{y1C})] + 0.749\sigma^4(v_{z1C}) + 0.0773 [\sigma^4(v_{x2C}) + \sigma^4(v_{y2C})] + 0.309\sigma^4(v_{z2C}) \\ & + 5.71 [\sigma^2(x_{1C}) \sigma^2(v_{x1C}) + \sigma^2(y_{1C}) \sigma^2(v_{y1C})] + 22.9\sigma^2(z_{1C}) \sigma^2(v_{z1C}) \\ & + 2.09 [\sigma^2(x_{2C}) \sigma^2(v_{x2C}) + \sigma^2(y_{2C}) \sigma^2(v_{y2C})] + 8.36\sigma^2(z_{2C}) \sigma^2(v_{z2C})\}, \end{aligned} \quad (47\text{a})$$

$$\begin{aligned} s(\Delta_s^{(C)} \phi) = & 4.92 [\sigma^2(x_{1C}) + \sigma^2(y_{1C})] - 9.84\sigma^2(z_{1C}) + 2.97 [\sigma^2(x_{2C}) + \sigma^2(y_{2C})] - 5.95\sigma^2(v_{z2C}) \\ & + 0.306 [\sigma^2(v_{x1C}) + \sigma^2(v_{y1C})] - 0.612\sigma^2(v_{z1C}) + 0.197 [\sigma^2(v_{x2C}) + \sigma^2(v_{y2C})] - 0.393\sigma^2(v_{z2C}), \end{aligned} \quad (47\text{b})$$

which for uncertainties (25a, 25b, 44) are equal to

$$\sigma(\Delta_s^{(C)} \phi) = 14\text{ppm}, \quad (48\text{a})$$

$$s(\Delta_s^{(C)} \phi) = 20\text{ppm}. \quad (48\text{b})$$

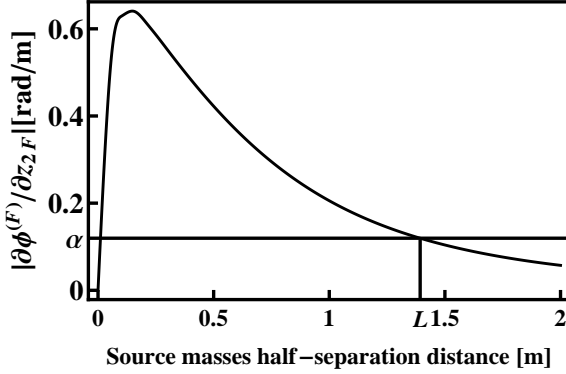


FIG. 5: Same as Fig. 3, but for 630 cylinders.

TABLE V: The same as Table III, but for the 630 cylinders.

Term	C-configuration	F-configuration
$\phi_s^{(T)}/\Delta_s^2\phi$	1.042989	-0.042989
Linear in position	$-9.65 \cdot 10^{-8}\delta z_{1C} + 1.33 \cdot 10^{-7}\delta z_{2C}$	$(3.30\delta z_{1F} - 3.41\delta z_{2F}) \cdot 10^{-2}$
Linear in velocity	$-1.86 \cdot 10^{-8}\delta v_{z1C} + 1.23 \cdot 10^{-7}\delta v_{z2C}$	$(8.03\delta v_{z1F} - 8.28\delta v_{z2F}) \cdot 10^{-3}$
Nonlinear in position	$5.13(\delta x_{1C}^2 + \delta y_{1C}^2) - 10.3\delta z_{1C}^2 + 3.10(\delta x_{2C}^2 + \delta y_{2C}^2) - 6.21\delta z_{2C}^2$	$(-33.5\delta x_{1F}^2 + 9.01\delta y_{1F}^2 - 1.63\delta x_{1F}\delta y_{1F} + 24.5\delta z_{1F}^2 - 32.8\delta x_{2F}^2 + 8.76\delta y_{2F}^2 - 1.60\delta x_{2F}\delta y_{2F} - 24.0\delta z_{2F}^2)$
Nonlinear in velocity	$0.319(\delta v_{x1C}^2 + \delta v_{y1C}^2) - 0.638\delta v_{z1C}^2 + 0.205(\delta v_{x2C}^2 + \delta v_{y2C}^2) - 0.410\delta v_{z2C}^2$	$(23.2\delta v_{x1F}^2 - 6.28\delta v_{y1F}^2 - 16.9\delta v_{z1F}^2 + 1.13\delta v_{x1F}\delta v_{y1F} + 22.3\delta v_{x2F}^2 - 5.94\delta v_{y2F}^2 + 1.09\delta v_{x2F}\delta v_{y2F} - 16.3\delta v_{z2F}^2) \cdot 10^{-4}$
Position-velocity cross term	$2.49(\delta v_{x1C}\delta x_{1C} + \delta v_{y1C}\delta y_{1C}) - 4.98\delta v_{z1C}\delta z_{1C} + 1.51(\delta v_{x2C}\delta x_{2C} + \delta v_{y2C}\delta y_{2C}) - 3.01\delta v_{z2C}\delta z_{2C}$	$[-163\delta v_{x1F}\delta x_{1F} + 43.9\delta v_{y1F}\delta y_{1F} - 3.97(\delta x_{1F}\delta v_{y1F} + \delta y_{1F}\delta v_{x1F}) + 119\delta v_{z1F}\delta z_{1F} - 159\delta v_{x2F}\delta x_{2F} + 42.5\delta v_{y2F}\delta y_{2F} - 3.88(\delta v_{x2F}\delta y_{2F} + \delta v_{y2F}\delta x_{2F}) + 117\delta v_{z2F}\delta z_{2F}] \cdot 10^{-4}$

Let us now consider the contribution from the F -configuration of the source mass. One determines the distance L of the halves of the source mass displacement in the horizontal direction from the inequality (34). The calculation showed that the greatest danger comes from the third term in braces in Eq. (33). Then one guarantees the inequality (34) fulfilment if

$$\left| \frac{\partial \phi^{(F)}(z_{2F}, v_{z2F})}{\partial z_{2F}} \right| \leq \alpha, \quad (49)$$

where

$$\alpha = \frac{\sqrt{0.21}\Delta_s\phi^{(C)}}{2\sigma(z_{2F})}\sigma(\Delta_s^{(C)}\phi) = 0.1195, \quad (50)$$

From Fig. 5 one sees that the halves of the source mass should be moved apart by a distance.

$$L = 1.39\text{m}. \quad (51)$$

Then, by computing the first order phase difference in the F -configuration, $\Delta_s\phi^{(F)}$, one obtains for the PDD

$$\Delta_s^2\phi = 3.51021\text{rad} \quad (52)$$

With this signal, the various relative contributions to the PDD are presented in the table V. Calculating from these data the first and second order derivatives with respect to the coordinates and velocities of the atomic clouds, and

substituting these derivatives in the equations (17), one receives

$$\begin{aligned}
\sigma \left(\Delta_s^{(2)} \phi \right) = & \{ 52.6 [\sigma^4(x_{1C}) + \sigma^4(y_{1C})] + 210\sigma^4(z_{1C}) + 19.3 [\sigma^4(x_{2C}) + \sigma^4(y_{2C})] + 77.0\sigma^4(z_{2C}) \\
& + 0.204 [\sigma^4(v_{x1C}) + \sigma^4(v_{y1C})] + 0.814\sigma^4(v_{z1C}) + 0.0841 [\sigma^4(v_{x2C}) + \sigma^4(v_{y2C})] \\
& + 0.336\sigma^4(v_{z2C}) + 6.21 [\sigma^2(x_{1C})\sigma^2(v_{x1C}) + \sigma^2(y_{1C})\sigma^2(v_{y1C})] + 24.9\sigma^2(z_{1C})\sigma^2(v_{z1C}) \\
& + 2.27 [\sigma^2(x_{2C})\sigma^2(v_{x2C}) + \sigma^2(y_{2C})\sigma^2(v_{y2C})] + 9.10\sigma^2(z_{2C})\sigma^2(v_{z2C}) \\
& + [1.09\sigma^2(z_{1F}) + 1.16\sigma^2(z_{2F})] \cdot 10^{-3} + [6.44\sigma^2(v_{z1F}) + 6.85\sigma^2(v_{z2F})] \cdot 10^{-5} \\
& + [2240\sigma^4(x_{1F}) + 162\sigma^4(y_{1F}) + 2.64\sigma^2(x_{1F})\sigma^2(y_{1F}) + 1200\sigma^4(z_{1F}) \\
& + 2150\sigma^4(x_{2F}) + 153\sigma^4(y_{2F}) + 2.56\sigma^2(x_{2F})\sigma^2(y_{2F}) + 1150\sigma^4(z_{2F})] \cdot 10^{-6} \\
& + [1080\sigma^4(v_{x1F}) + 78.8\sigma^4(v_{y1F}) + 1.28\sigma^2(v_{x1F})\sigma^2(v_{y1F}) + 575\sigma^4(v_{z1F}) \\
& + 993\sigma^4(v_{x2F}) + 70.6\sigma^4(v_{y2F}) + 1.18\sigma^2(v_{x2F})\sigma^2(v_{y2F}) + 534\sigma^4(v_{z2F})] \cdot 10^{-8} \\
& + [2650\sigma^2(x_{1F})\sigma^2(v_{x1F}) + 192\sigma^2(y_{1F})\sigma^2(v_{y1F}) + 1.57 (\sigma^2(y_{1F})\sigma^2(v_{x1F}) + \sigma^2(x_{1F})\sigma^2(v_{y1F})) \\
& + 1410\sigma^2(z_{1F})\sigma^2(v_{z1F}) + 2530\sigma^2(x_{2F})\sigma^2(v_{x2F}) + 181\sigma^2(y_{2F})\sigma^2(v_{y2F}) \\
& + 1.51 (\sigma^2(x_{2F})\sigma^2(v_{y2F}) + \sigma^2(y_{2F})\sigma^2(v_{x2F})) + 1360\sigma^2(z_{2F})\sigma^2(v_{z2F})] \cdot 10^{-7} \}^{1/2}, \tag{53a}
\end{aligned}$$

$$\begin{aligned}
s \left(\Delta_s^{(2)} \phi \right) = & 5.13 [\sigma^2(x_{1C}) + \sigma^2(y_{1C})] - 10.2\sigma^2(z_{1C}) + 3.10 [\sigma^2(x_{2C}) + \sigma^2(y_{2C})] - 6.22\sigma^2(z_{2C}) \\
& + 0.319 [\sigma^2(v_{x1C}) + \sigma^2(v_{y1C})] - 0.638\sigma^2(v_{z1C}) + 0.205 [\sigma^2(v_{x2C}) + \sigma^2(v_{y2C})] - 0.410\sigma^2(v_{z2C}) \\
& + [33.5\sigma^2(x_{1F}) + 9.01\sigma^2(y_{1F}) + 24.5\sigma^2(z_{1F}) 32.9\sigma^2(x_{2F}) + 8.75\sigma^2(y_{2F}) + 24.0\sigma^2(z_{2F})] \cdot 10^{-3} \\
& + [23.2\sigma^2(v_{x1F}) - 6.28\sigma^2(v_{y1F}) - 16.9\sigma^2(v_{z1F}) + 22.3\sigma^2(v_{x2F}) - 5.94\sigma^2(v_{y2F}) - 16.3\sigma^2(v_{z2F})] \cdot 10^{-4} \tag{53b}
\end{aligned}$$

At uncertainties (25a, 25b, 44), RSD and shift are equal to

$$\sigma \left(\Delta_s^{(2)} \phi \right) = 16 \text{ ppm}, \tag{54a}$$

$$s \left(\Delta_s^{(2)} \phi \right) = 20 \text{ ppm}. \tag{54b}$$

Note also that we have considered the displacement of the source mass as a whole in the vertical direction, and found that the minimal distance at this displacement is equal to

$$L = 2.92 \text{ m}. \tag{55}$$

This displacement is only 25% shorter than the displacement of the source mass by 4m required for the technique [13]. However, it is more than two times longer than the horizontal displacement (51). Therefore, in the case of a 13-ton source mass, horizontal displacement is preferable.

VII. CONCLUSION

This article is devoted to the calculation of the error budget in the measurement of the Newtonian gravitational constant G by atomic interferometry methods. Using the technique [20], we obtained expressions for the gravitational field of the cylinder, which is used in these measurements.

Despite the compensation of the gradient of the Earth gravitational field at the points of apogees of the atomic trajectories achieved in the article [3, 4], an absence of this compensation along the entire trajectory leads to the influence of the Earth's field on the G measurement accuracy. To overcome this influence, we propose to use the method of eliminating the gradient of the gravitational field of the Earth [12].

The main attention in this article is paid to the calculation of standard deviation (SD) and the shift of the PDD due to the uncertainties of the mean values of the initial coordinates and the velocities of atomic clouds $\{\delta \mathbf{x}, \delta \mathbf{v}\}$. We propose to include in the error budget new terms. They are originated from the quadratic dependence of the variation of the AI phases on $\{\delta \mathbf{x}, \delta \mathbf{v}\}$. The shift arises only after including those terms. At the conditions realized in the article [3, 4], calculations bring us to the shift (26b) and to the opposite relative correction $\Delta G/G = -199 \text{ ppm}$,

which is larger than corrections considered in [3, 4]. After including this correction, the value of the gravitational constant G should be shifted to

$$G = 6.67058 \text{m}^3 \text{kg}^{-1} \text{s}^{-2} \quad (56)$$

from the value $G = 6.67191 \text{m}^3 \text{kg}^{-1} \text{s}^{-2}$ measured in [3, 4].

After eliminating the gradient of the Earth field, one can use optimization technique proposed in [5, 10]. While the PDD in this case becomes smaller [compare signals (23) and (29)], one should be able to measure G with 2.75 times better accuracy [compare RSDs (26a) and (41a)].

Another application of our formulas is the calculation of the systematic error due to the finite size of atomic clouds and their finite temperature [5, 10]. Let us now assume that $\delta\mathbf{x}$ is the deviation of the atom from the center of the cloud and $\delta\mathbf{v}$ is the deviation from the center of the atomic velocity distribution. If the temperatures are small enough to ignore the Doppler frequency shift, and the aperture of the optical field is large enough to assume that the areas of the Raman pulses do not depend on the position of atoms in the cloud, then the only reason for the dependence of the PDD on $\{\delta\mathbf{x}, \delta\mathbf{v}\}$ is that the gravitational field $\delta\mathbf{g}[\mathbf{x}(t)]$ is not the same for different atoms in the cloud. Averaging the phase of the AI over an atomic distribution one will receive from the equation (13)

$$\langle \delta\phi \rangle = \frac{1}{4} \left(a_m^2 \frac{\partial^2 \phi}{\partial x_m^2} + v_{0m}^2 \frac{\partial^2 \phi}{\partial v_m^2} \right), \quad (57)$$

where $a_m = \sqrt{2 \langle \delta x_m^2 \rangle}$ and $v_{0m} = \sqrt{2 \langle \delta v_m^2 \rangle}$ are the radius and thermal velocity of the atomic cloud along the m -axis. Here we pay attention to the fact that at equal radii, $a_x = a_y = a_z$, and temperatures, $v_{0x} = v_{0y} = v_{0z}$, the systematic error (57) disappears. This follows from the Eqs. (21c, 21e) and from the fact that the gravitational field obeys the Laplace equation and, therefore, the trace of the gravitational field curvature tensor (22) $\chi_{zmm} = 0$.

In the absence of linear terms, one can diagonalize the quadratic shape in phase variation (13), so that.

$$\delta\phi = \sum_{m=1}^6 a_m \delta q_m^2. \quad (58)$$

By analogy with the error budget in [2–4, 13, 14, 18, 21], if each term m in Eq. (58) is independent of the others, one might expect that his contribution to the SD is

$$\sigma_m(\phi) = |a_m| \sigma^2(q_m), \quad (59)$$

and

$$\sigma(\phi) = \left[\sum_{m=1}^6 \sigma_m^2(\phi) \right]^{1/2}. \quad (60)$$

This, however, is not precisely correct. The calculation shows that for independent extreme variables, the expression (60) is true, but the contribution of each term is

$$\sigma_m(\phi) = \sqrt{2} |a_m| \sigma^2(q_m) \left(1 + \frac{1}{2} \kappa(q_m) \right)^{1/2}, \quad (61)$$

where $\kappa(q_m)$ is a cumulant (16), i.e. even for normal distribution, when $\kappa(q_m) = 0$, the contribution from each term is $\sqrt{2}$ times greater than in (59).

Instead of using tables, we propose to use for error budget expressions for relative SD (24a, 31a, 40a, 47a, 53a) and relative shift (24b, 31b, 40b, 47b, 53b) [obtained by means of general Eqs. (17)], in which one should substitute the coordinates and velocities uncertainties achieved or assumed to be achieved in the experiment.

In this article we have only considered error budget related to atomic variables and did not consider errors associated with the properties of the source mass. Examples of calculation errors associated with the uncertainties of positioning and orientation of the various components of the source mass can be found in the article [10]. We would only like to emphasize that, as in the article [13], it is preferable to use source masses consisting of as many components as possible. So if one uses N cylinders, the signal f consists of the contributions f_m of the each cylinder ($m = 1, \dots, N$).

For RSD one gets $\sigma_r(f) = \left[\sum_m f_m^2 \sigma_r^2(f_m) \right]^{1/2} / f$. If one accepts for estimates that the contributions of the various

cylinders and their RSDs are of the same order, $f_m \sim f_{m'} \sim f/N$ and $\sigma_r(f_m) \sim \sigma_r(f_{m'})$, then we get that the RSD of the entire system of cylinders decreases as $N^{-1/2}$,

$$\sigma_r(f) \sim N^{-1/2} \sigma_r(f_m). \quad (62)$$

Finally, we would like to note that, following the statement [13], that 13-ton source mass can be implemented in the experiment, we increased the number of cylinders to 630 (more than 26 times). At the same time, the optimal signal increased only 8.4 times [compare Eqs. (52) and (39)], and this increase is partly due to an increase in the delay time between the Raman pulses T . This example shows that an increase in the weight of the source mass does not even lead to a proportional signal increase. More promising here is an increase in the signal due to the large values of T , the effective wave vector k and the optimal aspect ratio of the source mass. Due to these factors we predicted [5] PDD $\Delta_s^{(2)}\phi = 386.527\text{rad}$ even for a source mass $M = 1080\text{kg}$.

Acknowledgments

Author is appreciated to Dr. M. Prevedeli for the fruitful discussions and to Dr. G. Rosi for the explanation of some points in the article [13].

Appendix A: Gravity field of the homogeneous cylinder

1. Axial component

It is convenient [20] to explore the following expression for the potential of the gravitational field of a homogeneous cylinder $\Phi(\mathbf{x})$

$$\Phi(r, z) = -2G\rho \int_0^R dy \int_{r-\sqrt{R^2-y^2}}^{r+\sqrt{R^2-y^2}} d\xi \int_{z-h}^z \frac{d\zeta}{\sqrt{y^2 + \xi^2 + \zeta^2}}, \quad (A1)$$

where ρ , R , and h are the density, radius, and height of the cylinder, $(r, z, \psi = 0)$ are the cylindrical coordinates of the vector \mathbf{x} . For an axial component of the gravitational field, $\delta g_z(r, z) = -\partial_z \Phi(r, z)$, one gets

$$\delta g_z(r, z) = 2G\rho g_z(r, \zeta) \Big|_{\zeta=z-h}^{\zeta=z}, \quad (A2)$$

where the function

$$g_z(r, \zeta) = \int_0^R dy \int_{r-\sqrt{R^2-y^2}}^{r+\sqrt{R^2-y^2}} \frac{d\xi}{\sqrt{y^2 + \xi^2 + \zeta^2}} \quad (A3)$$

can be represented as

$$\begin{aligned} g_z(r, \zeta) &= \int_0^R dy \ln \frac{t_+(y)}{t_-(y)} \\ &= - \int_0^R y \left(\frac{dt_+}{t_+} - \frac{dt_-}{t_-} \right), \end{aligned} \quad (A4a)$$

$$t_{\pm}(y) = r \pm \sqrt{R^2 - y^2} + \left(\zeta^2 + r^2 + R^2 \pm 2r\sqrt{R^2 - y^2} \right)^{1/2} \quad (A4b)$$

Since $t_+(R) = t_-(R) \equiv t(R) \leq t_{\pm}(0)$ one can write

$$g_z(r, \zeta) = \int_{t(R)}^{t_{\pm}(0)} \frac{dt}{t} y_+(t) + \int_{t_{\pm}(0)}^{t(R)} \frac{dt}{t} y_-(t), \quad (A5)$$

where $y_{\pm}(t)$ is the root of the equation $t_{\pm}(y) = t$. To find this root, consider the functions $x_{\pm}(t) = \sqrt{R^2 - y_{\pm}^2(t)}$,

$$0 < x_{\pm}(t) < R. \quad (A6)$$

For them one gets

$$x_{\pm}(t) = \pm t + \sqrt{\zeta^2 + R^2 + 2tr} \text{ or } \pm t - \sqrt{\zeta^2 + R^2 + 2tr} \quad (\text{A7})$$

Since $t + \sqrt{\zeta^2 + R^2 + 2tr} > R$, then one should choose $x_+(t) = t - \sqrt{\zeta^2 + R^2 + 2tr}$. Since $t_-(0) > r - R + |r - R| > 0$, $-t - \sqrt{\zeta^2 + R^2 + 2tr} < 0$, hence $x_-(t) = \sqrt{\zeta^2 + R^2 + 2tr} - t$ or

$$x_{\pm}(t) = \pm \left(t - \sqrt{\zeta^2 + R^2 + 2tr} \right). \quad (\text{A8})$$

Therefore, one concludes that the functions $y_{\pm}(t)$ are coincident and equal to

$$y_+(t) = y_-(t) = y(t) = \left[2t \left(\sqrt{\zeta^2 + R^2 + 2tr} - r \right) - t^2 - \zeta^2 \right]^{1/2} \quad (\text{A9})$$

and.

$$g_z(r, \zeta) = \int_{t_-(0)}^{t_+(0)} \frac{dt}{t} y(t). \quad (\text{A10})$$

Introducing new variable,

$$u = \sqrt{\zeta^2 + R^2 + 2tr} - r, \quad (\text{A11})$$

for which

$$u[t_{\pm}(0)] \equiv u_{\pm} = \sqrt{\zeta^2 + (r \pm R)^2}, \quad (\text{A12a})$$

$$y(t) = \frac{\sqrt{q(u^2)}}{2r}, \quad (\text{A12b})$$

$$q(\eta) = \{u_+^2 - \eta\} \{\eta - u_-^2\}, \quad (\text{A12c})$$

$$dt = \frac{u+r}{r} du \quad (\text{A12d})$$

and so

$$g_z(r, \zeta) = I + I', \quad (\text{A13a})$$

$$I = \int_{u_-}^{u_+} \frac{du}{\sqrt{q(u^2)}} J(u), \quad (\text{A13b})$$

$$J(u) = \frac{q(u^2) (r^2 - \zeta^2 - R^2 - u^2)}{w(u^2)}, \quad (\text{A13c})$$

$$I' = \frac{1}{2r} \int_{u_-^2}^{u_+^2} d\eta J'(\eta), \quad (\text{A13d})$$

$$J'(\eta) = \frac{(\eta - \zeta^2 - R^2 - r^2)}{\sqrt{q(\eta)} w(\eta)}, \quad (\text{A13e})$$

$$w(\eta) = (\eta - \eta_1)(\eta - \eta_2), \quad (\text{A13f})$$

$$\eta_{1,2} = \left(r \pm \sqrt{\zeta^2 + R^2} \right)^2. \quad (\text{A13g})$$

Using equality

$$w(\eta) + q(\eta) = -4r^2 \zeta^2, \quad (\text{A14})$$

one can show that the integrand $J'(\eta)$ is an antisymmetric function with respect to the middle point $\eta = \{u^2[t_+(0)] + u^2[t_-(0)]\}/2$, and, therefore, the term (A13d) is equal 0. At the same time, expanding $J(u)$ into

partial fractions, one obtains

$$g_z(r, \zeta) = (R^2 + \zeta^2 - r^2) I_1 + I_2 + I_{3+} + I_{3-}, \quad (\text{A15a})$$

$$I_1 = \int_{u_-}^{u_+} \frac{du}{\sqrt{q(u^2)}}, \quad (\text{A15b})$$

$$I_2 = \int_{u_-}^{u_+} \frac{du u^2}{\sqrt{q(u^2)}}, \quad (\text{A15c})$$

$$I_{3\pm} = 2r\zeta^2 \left(r \pm \sqrt{\zeta^2 + R^2} \right) \int_{u_-}^{u_+} \frac{du}{\sqrt{q(u^2)} (u^2 - \eta_{1,2})} \quad (\text{A15d})$$

The integrals (A15), one can compute using the substitution

$$u = \sqrt{u_+^2 - (u_+^2 - u_-^2) \sin^2 \phi} \quad (\text{A16})$$

Finally, one arrives at the following expression for the axial component of the cylinder's field

$$\delta g_z(r, z) = 2G\rho g_z(r, \zeta) \zeta^{\zeta=z}_{\zeta=z-h}, \quad (\text{A17a})$$

$$g_z(r, \zeta) = \frac{(\zeta^2 + R^2 - r^2)}{\sqrt{\zeta^2 + (r+R)^2}} K \left(\frac{4rR}{\zeta^2 + (r+R)^2} \right) + \sqrt{\zeta^2 + (r+R)^2} E \left(\frac{4rR}{\zeta^2 + (r+R)^2} \right) + \frac{\zeta^2}{\sqrt{\zeta^2 + (r+R)^2}} \sum_{j=\pm 1} \left[\frac{r + j\sqrt{\zeta^2 + R^2}}{R - j\sqrt{\zeta^2 + R^2}} \Pi \left(\frac{2R}{R - j\sqrt{\zeta^2 + R^2}} \mid \frac{4rR}{\zeta^2 + (r+R)^2} \right) \right], \quad (\text{A17b})$$

where $K(k)$, $E(k)$ and $\Pi(\alpha|k)$ are the complete elliptic integrals of the first, second and third order respectively.

2. Radial component

For the radial component of the gravitational field $\delta g_r(r, z) = -\partial_r \Phi(r, z)$ one obtains from (A1)

$$\delta g_r(r, z) = 2G\rho g_r(r, \zeta) \zeta^{\zeta=z}_{\zeta=z-h}, \quad (\text{A18a})$$

$$g_r(r, \zeta) = - \int_0^R y \left(\frac{dt_+}{t_+} - \frac{dt_-}{t_-} \right), \quad (\text{A18b})$$

$$t_{\pm}(y) = \zeta + \left[\zeta^2 + r^2 + R^2 \pm 2r\sqrt{R^2 - y^2} \right]^{1/2} \quad (\text{A18c})$$

Since still $t_+(R) = t_-(R) \leq t_{\pm}(0)$, one gets,

$$g_r(r, \zeta) = \int_{t_-(0)}^{t(R)} \frac{dt}{t} y_-(t) + \int_{t(R)}^{t_+(0)} \frac{dt}{t} y_+(t), \quad (\text{A19})$$

where $y_{\pm}(t)$ are functions inverse to (A18c). Since these functions are the same

$$y_+(t) = y_-(t) \equiv y(t) = \frac{1}{2r} \left[4r^2 R^2 - (t^2 - 2\zeta t - r^2 - R^2)^2 \right]^{1/2}, \quad (\text{A20})$$

then, choosing as an integration variable $u = t - \zeta$, one finds that

$$g_r(r, \zeta) = I + I', \quad (\text{A21a})$$

$$I = -\frac{\zeta}{2r} \int_{u_-}^{u_+} \frac{du q(u^2)}{(u^2 - \zeta^2) \sqrt{q(u^2)}}, \quad (\text{A21b})$$

$$I' = \frac{1}{4r} \int_{u_-^2}^{u_+^2} \frac{d\eta \sqrt{q(\eta)}}{(\eta - \zeta^2)}, \quad (\text{A21c})$$

where u_{\pm} and $q(\eta)$ are given by Eqs. (A12a, A12c). Because $u_{\pm}^2 - \zeta^2$ and $q(\eta + \zeta^2)$ are independent of ζ , the term I' gives no contribution to the acceleration (A18a) and can be omitted. While using the substitution (A16), one reduces the integral in (A21b) to elliptic integrals, which brings us to the next final result

$$\delta g_r(r, z) = 2G\rho g_r(r, \zeta)_{\zeta=z-h}^{\zeta=z}, \quad (\text{A22a})$$

$$g_r(r, \zeta) = \frac{\zeta}{2r\sqrt{\zeta^2 + (r+R)^2}} \left[-(\zeta^2 + 2r^2 + 2R^2) K\left(\frac{4rR}{\zeta^2 + (r+R)^2}\right) \right. \\ \left. + (\zeta^2 + (r+R)^2) E\left(\frac{4rR}{\zeta^2 + (r+R)^2}\right) + \frac{(r^2 - R^2)^2}{(r+R)^2} \Pi\left(\frac{4rR}{(r+R)^2} \mid \frac{4rR}{\zeta^2 + (r+R)^2}\right) \right]. \quad (\text{A22b})$$

[1] B. Ya. Dubetskii, A. P. Kazantsev, V. P. Chebotayev, V. P. Yakovlev, Interference of atoms and formation of atomic spatial arrays in light fields, Pis'ma Zh. Eksp. Teor. Fiz. **39**, 531 (1984) [JETP Lett. **39**, 649 (1984)].

[2] J. B. Fixler, G. T. Foster, J. M. McGuirk, M. A. Kasevich, Atom Interferometer Measurement of the Newtonian Constant of Gravity, Science **315**, 74 (2007).

[3] G. Rosi, F. Sorrentino, L. Cacciapuoti, M. Prevedelli & G. M. Tino, Precision measurement of the Newtonian gravitational constant using cold atoms, Nature **510**, 518 (2014).

[4] G. Rosi, F. Sorrentino, L. Cacciapuoti, M. Prevedelli & G. M. Tino, Precision measurement of the Newtonian gravitational constant using cold atoms, arXiv:1412.7954 [physics.atom-ph].

[5] B. Dubetsky, Atom interferometers' phases at the presence of heavy masses; their use to measure Newtonian gravitational constant; optimization, error model, perspectives, In Proceedings of the MPLP-2016 Conference, Novosibirsk, Russia, 2016, IOP Conf. Series: Journal of Physics: Conf. Series **793** 012006 (2017).

[6] S. M. Dickerson, J. M. Hogan, A. Sugarbaker, D. M. S. Johnson, M. A. Kasevich, Multi-axis inertial sensing with long-time point source atom interferometry, Phys. Rev. Lett. **111**, 083001 (2013).

[7] T. Kovachy, J. M. Hogan, A. Sugarbaker, S. M. Dickerson, C. A. Donnelly, C. Overstreet, and M. A. Kasevich, Matter Wave Lensing to Picokelvin Temperatures, Phys. Rev. Lett. **114** 143004 (2015).

[8] T. Kovachy, P. Asenbaum, C. Overstreet, C. A. Donnelly, S. M. Dickerson, A. Sugarbaker, J. M. Hogan & M. A. Kasevich, Nature **528**, 530 (2015).

[9] G. W. Biedermann, X. Wu, L. Deslauriers, S. Roy, C. Mahadeswaraswamy, M. A. Kasevich, Testing Gravity with Cold-Atom Interferometers, Phys. Rev. A **91**, 033629 (2015).

[10] B. Dubetsky, Optimization and error model for atom interferometry technique to measure Newtonian gravitational constant, arXiv:1407.7287v2 [physics.atom-ph].

[11] M. J. Snadden, J. M. McGuirk, P. Bouyer, K. G. Haritos, and M. A. Kasevich, Measurement of the Earth's Gravity Gradient with an Atom Interferometer-Based Gravity Gradiometer, Phys. Rev. Lett. **81**, 971 (1998).

[12] A. Roura, Circumventing Heisenberg's uncertainty principle in atom interferometry tests of the equivalence principle, Phys. Rev. Lett. **118**, 160401 (2017).

[13] G. Rosi, A proposed atom interferometry determination of G at 10^{-5} using a cold atomic fountain, Metrologia **55**, 50 (2018).

[14] A. Peters, K. Y. Chung and S. Chu, High-precision gravity measurements using atom interferometry, Metrologia **38**, 25 (2001).

[15] M. Schmidt, A mobile high-precision gravimeter based on atom interferometry, Mathematisch-Naturwissenschaftlichen Fakultät I der Humboldt-Universität zu Berlin, Thesis (2011), p. 109.

[16] M. Prevedelli, L. Cacciapuoti, G. Rosi, F. Sorrentino and G. M. Tino, Measuring the Newtonian constant of gravitation G with an atomic interferometer, Phil. Trans. R. Soc. A **372**, 20140030 (2014).

[17] M. A. Kasevich and B. Dubetsky, Kinematic Sensors Employing Atom Interferometer Phases, US Patent 7,317,184 (2005).

[18] G. Lamporesi, Determination of the gravitational constant by atom interferometry, Thesis, University of Florence, 2006.

[19] Z. F. Seidov, P. I. Skvirsky, arXiv:astro-ph/0002496v1.

[20] Y. T. Chen, A. Cook, Gravitational experiment in the laboratory, Cambridge University Press, Cambridge 1993.

[21] A. Peters, K. Y. Chung, and S. Chu, Measurement of gravitational acceleration by dropping atoms, Nature, **400**, 849 (1999).

[22] A. M. Mathai, S. B. Provost, Quadratic forms in random variables: theory and applications, Marcel Dekker, INC, New York, 1993.

[23] B. Dubetsky, Full elimination of the gravity-gradient terms in atom interferometry, Appl. Phys. B **125**, 187 (2019).

[24] B. Dubetsky, S. B. Libby and P. Berman, Atom interferometry in the presence of an external test mass, Atoms, **4**, 14 (2016).

[25] P. J. Mohr, D. B. Newell, B. N. Taylor, CODATA Recommended Values of the Fundamental Physical Constants: 2014, Rev. Mod. Phys., **88**, 035009 (2016).

- [26] M. de Angelis, F. Greco, A. Pistorio, N. Poli, M. Prevedelli, G. Saccorotti, F. Sorrentino, and G. M. Tino, Measurement of absolute gravity acceleration in Firenze, *Solid Earth Discuss.* **3**, 43 (2011).
- [27] M. P. Bradley, J. V. Porto, S. Rainville, J. K. Thompson, and D. E. Pritchard, Penning Trap Measurements of the Masses of ^{133}Cs , $^{87,85}\text{Rb}$, and ^{23}Na with Uncertainties <0.2 ppb, *Phys. Rev. Lett.* **83**, 4510 (1999).
- [28] R. G. Beausoleil, T. W. Hansch, Ultra-high resolution two-photon optical Ramsey spectroscopy of an atomic fountain, *Phys. Rev. A* **33**, 1661 (1986).